Multi-relaxation-time lattice Boltzmann front tracking method for two-phase flow with surface tension*

Xie Hai-Qiong(谢海琼)[a], Zeng Zhong(曾 忠)[a)b)c)†], Zhang Liang-Qi(张良奇)[a], Liang Gong-You(梁功有)[a], Hiroshi Mizuseki[c], and Yoshiyuki Kawazoe[c]

[a] *Department of Engineering Mechanics, Chongqing University, Chongqing* 400044, *China*

[b] *State Key Laboratory of Coal Mine Disaster Dynamics and Control, Chongqing University, Chongqing* 400044, *China*

[c] *Institute for Materials Research, Tohoku University, Sendai* 980-8577, *Japan*

(Received 11 May 2012; revised manuscript received 5 June 2012)

In this paper, an improved incompressible multi-relaxation-time lattice Boltzmann-front tracking approach is proposed to simulate two-phase flow with a sharp interface, where the surface tension is implemented. The lattice Boltzmann method is used to simulate the incompressible flow with a stationary Eulerian grid, an additional moving Lagrangian grid is adopted to track explicitly the motion of the interface, and an indicator function is introduced to update the fluid properties accurately. The interface is represented by using a four-order Lagrange polynomial through fitting a set of discrete marker points, and then the surface tension is directly computed by using the normal vector and curvature of the interface. Two benchmark problems, including Laplace's law for a stationary bubble and the dispersion relation of the capillary wave between two fluids are conducted for validation. Excellent agreement is obtained between the numerical simulations and the theoretical results in the two cases.

Keywords: lattice Boltzmann method, multi-relaxation-time, front tracking method, surface tension, two-phase flow

PACS: 47.61.Jd, 47.11.–j, 47.45.Ab **DOI:** 10.1088/1674-1056/21/12/124703

1. Introduction

The immiscible two-phase flows with a sharp interface often appear in nature and many industrial processes, such as water waves, coating flow, bubble dynamics in chemical reactors, surface tension-driven flow, free surface deformation in the crystal growth process, and so on. Owing to the practical importance for the processes involving multi-phase flow with surface tension and also its challenge in numerical simulation, they attract many studies in the field, and a number of different methods based on traditional fluid dynamics, including the finite difference method, the finite volume method, and the finite element method, have been developed to simulate and predict the behaviors of such flows.[1−3]

The lattice Boltzmann method (LBM) has been developed as an alternative numerical scheme for modeling complex fluid dynamics problems. The main advantages attributed to the LBM are the simplicity in programming and the ease of parallelization.[4] Recently, the LBM has been widely adopted to simulate multiphase flow,[5−7] fluid-structure interaction,[8−10] and thermal fluid flows.[11,12]

In the LBM framework, several kinds of multiphase fluid models have already been developed and used to simulate multiphase flow. The first immiscible multiphase LBM model was proposed by Gunstensen *et al.*[5] It contains two sets of LBM distribution functions, one for each phase, and through the repulsive interaction based on the colour gradient the phase separation is achieved. The second model, the so-called pseudo-potential model, was proposed by Shan and Chen,[6] who introduced the concept of interaction potentials. Swift *et al.*[7] proposed a free energy model; it also relies on a second set of distribution functions which describes the fluid fraction and is determined by the free energy of the system.

The above-mentioned multiphase LBM models belong to diffusive interface capturing methods, and these models all rely on an implicit description of the interface. Recently, Lallemand *et al.*[13] proposed a

*Project supported by the National Natural Science Foundation of China (Grant Nos. 10872222 and 50921063), the Specialized Research Fund for the Doctoral Program of Higher Education of China (Grant No. 20110191110037), and the Fundamental Research Funds for the Central Universities, China (Grant Nos. CDJXS11240011 and CDJXS10241103).

†Corresponding author. E-mail: zzeng@cqu.edu.cn

hybrid method combining the LBM and the front-tracking method. The basic idea behind the front tracking method, using a set of connected discrete marker points to track explicitly the interface motion, is intuitive and fairly simple. These computational Lagrangian marker points are independent of the background Eulerian mesh. At each time step, information is exchanged between the moving Lagrangian marker points and the stationary Eulerian mesh points, and this information exchange is achieved by using Peskin's immersed boundary method.[14]

In this paper, the front tracking method[15,16] is used on the basis of He and Luo's incompressible LBM,[17] by combining these two methods, and we develop a model to study two-phase flow with sharp dynamical interface and surface tension. For two-phase flow, the fluids separated by the interface are treated as one fluid with varying physical properties. Furthermore, an indicator function $I(\boldsymbol{x},t)$ is introduced, and its value is taken to be 1 in one phase and 0 in the other phase. According to this indicator function, the entire fluid with varying physical properties is immediately updated, in the meantime, the surface tension is directly computed at the interface. In order to improve the numerical stability of the single-relaxation-time LBM, we further develop He and Luo's LBM model by using a multi-relaxation-time LBM technique. To verify the ability and accuracy of the model for two-phase flow, two benchmarks, including Laplace's law for a stationary bubble and the dispersion relation of the capillary wave between two fluids, are performed.

2. Numerical methods

Our algorithm consists of three major parts: the flow solver, the interface tracking, and the computation of the surface tension. The flow solver is developed based on an incompressible multi-relaxation-time LBM; the front tracking method is adopted to track the dynamical interface; and the surface tension is computed directly on the interface.

2.1. Lattice Boltzmann method

The D2Q9 model, a widely used LBM model for two-dimensional flow, is adopted in this paper. The discrete lattice Boltzmann equation is

$$\begin{aligned} &f_\alpha(\boldsymbol{x}+\boldsymbol{e}_\alpha\delta_t, t+\delta_t) - f_\alpha(\boldsymbol{x},t) \\ &= -\frac{1}{\tau}[f_\alpha(\boldsymbol{x},t) - f_\alpha^{(\mathrm{eq})}(\boldsymbol{x},t)], \end{aligned} \tag{1}$$

where $f_\alpha(\boldsymbol{x},t)$ is the distribution function for particles with velocity e_α at position $\boldsymbol{x}$ and time t, and $f_\alpha^{(\mathrm{eq})}(\boldsymbol{x},t)$ is the equilibrium distribution function. The dimensionless relaxation parameter τ is related to the speed of sound c_s and kinematic viscosity ν by $\nu = c_s^2(\tau - 1/2)\delta_t$, where $c_s = \sqrt{1/3}\delta_x/\delta_t$, and δ_x and δ_t are the lattice space and time step, respectively.

The discrete velocities read

$$\boldsymbol{e}_\alpha = \begin{cases} (0,0), & \alpha = 0, \\ (\cos[(\alpha-1)\pi/2], \sin[(\alpha-1)\pi/2])\, c, & \alpha = 1-4, \\ (\cos[(2\alpha-9)\pi/4], \sin[(2\alpha-9)\pi/4])\, \sqrt{2}c, & \alpha = 5-8, \end{cases} \tag{2}$$

where $c = \delta_x/\delta_t$ is the lattice velocity.

For the incompressible LBM model,[17] the discrete equilibrium distribution function is defined as

$$\begin{aligned} f_\alpha^{(\mathrm{eq})}(\boldsymbol{x},t) = \omega_\alpha \Bigg\{ \delta\rho + \rho_0 \Bigg[3\frac{(\boldsymbol{e}_\alpha\cdot\boldsymbol{u})}{c_s^2} \\ + \frac{9}{2}\frac{(\boldsymbol{e}_\alpha\cdot\boldsymbol{u})^2}{c_s^4} - \frac{3}{2}\frac{\boldsymbol{u}^2}{c_s^2} \Bigg] \Bigg\}, \end{aligned} \tag{3}$$

where $\delta\rho$ is the fluctuation density, ρ_0 is the initiation density, and the weighting coefficients ω_α are

$$\omega_\alpha = \begin{cases} \dfrac{4}{9}, & \alpha = 0, \\ \dfrac{1}{9}, & \alpha = 1,2,3,4, \\ \dfrac{1}{36} & \alpha = 5,6,7,8. \end{cases} \tag{4}$$

The fluid macroscopic fluctuation density $\delta\rho$ and velocity $\boldsymbol{u}$ are computed from the moments of the distribution functions as follows:[17]

$$\delta\rho = \sum_\alpha f_\alpha, \tag{5}$$

$$\boldsymbol{u} = \frac{1}{\rho_0}\sum_\alpha \boldsymbol{e}_\alpha f_\alpha. \tag{6}$$

The above LBM model is based on the BGK col-

lision approximation. It is known that numerical instability may appear in this model, and therefore, a multi-relaxation-time collision technique is introduced to improve the numerical stability. The evolution equation is expressed as

$$\begin{aligned} & f_\alpha(\boldsymbol{x}+\boldsymbol{e}_\alpha\delta_t, t+\delta_t) - f_\alpha(\boldsymbol{x}, t) \\ = & -S_{\alpha i}[f_i(\boldsymbol{x}, t) - f_i^{(\mathrm{eq})}(\boldsymbol{x}, t)], \end{aligned} \tag{7}$$

where $S_{\alpha i}$ is the component of the collision matrix $\boldsymbol{S}$. In the velocity space, the full matrix $\boldsymbol{S}$ results in the difficulty in implementing the collision step. Based on the ideas in Refs. [18] and [19], the full collision matrix in the moment space can be transformed into a diagonal matrix, which leads to much convenience in performing the collision process. Therefore, equation (7) is transformed as

$$\begin{aligned} & \boldsymbol{f}(\boldsymbol{x}+\boldsymbol{e}_\alpha\delta_t, t+\delta_t) - \boldsymbol{f}(\boldsymbol{x}, t) \\ = & -\boldsymbol{M}^{-1}\tilde{\boldsymbol{S}}[\boldsymbol{m}(\boldsymbol{x}, t) - \boldsymbol{m}^{(\mathrm{eq})}(\boldsymbol{x}, t)], \end{aligned} \tag{8}$$

where $\boldsymbol{m}(\boldsymbol{x}, t)$ and $\boldsymbol{m}^{(\mathrm{eq})}(\boldsymbol{x}, t)$ are moments and their corresponding equilibria, and $\tilde{\boldsymbol{S}}$ is a diagonal matrix whose components represent the relaxation time of the moments

$$\begin{aligned} \tilde{\boldsymbol{S}} &= \boldsymbol{M}\boldsymbol{S}\boldsymbol{M}^{-1} \\ &= \mathrm{diag}\,(s_0, s_1, s_2, s_3, s_4, s_5, s_6, s_7, s_8)\,. \end{aligned} \tag{9}$$

The transformation between the velocity space and moment space is achieved by the matrix $\boldsymbol{M}$, which serves as a transformation matrix, and maps the distribution functions $f(\boldsymbol{x}, t)$ to their moments

$$\begin{aligned} \boldsymbol{m} &= \boldsymbol{M}\boldsymbol{f}, \\ \boldsymbol{f} &= \boldsymbol{M}^{-1}\boldsymbol{m}. \end{aligned} \tag{10}$$

The transformation matrix $\boldsymbol{M}$, which can be constructed via the Gram–Schmidt orthogonalization procedure from some polynomials of the components of the discrete velocities,[18] is expressed as

$$\boldsymbol{M} = \begin{pmatrix} 1 & 1 & 1 & 1 & 1 & 1 & 1 & 1 & 1 \\ -4 & -1 & -1 & -1 & 2 & 2 & 2 & 2 & 2 \\ 4 & -2 & -2 & -2 & -2 & 1 & 1 & 1 & 1 \\ 0 & 1 & 0 & -1 & 0 & 1 & -1 & -1 & 1 \\ 0 & -2 & 0 & 2 & 0 & 1 & -1 & -1 & 1 \\ 0 & 0 & 1 & 0 & -1 & 1 & 1 & -1 & -1 \\ 0 & 0 & -2 & 0 & 2 & 1 & 1 & -1 & -1 \\ 0 & 1 & -1 & 1 & -1 & 0 & 0 & 0 & 0 \\ 0 & 0 & 0 & 0 & 0 & 1 & -1 & 1 & -1 \end{pmatrix}. \tag{11}$$

Based on the equilibrium distribution function of an incompressible single-relaxation-time LBM model, as indicated in Eq. (3), the corresponding equilibrium moments are obtained by $\boldsymbol{m}^{(\mathrm{eq})} = \boldsymbol{M}\boldsymbol{f}^{(\mathrm{eq})}$

$$m_0^{(\mathrm{eq})} = \delta\rho, \quad m_1^{(\mathrm{eq})} = -2\delta\rho + 3\boldsymbol{j}\cdot\boldsymbol{j}\,/\rho_0, \tag{12a}$$

$$m_2^{(\mathrm{eq})} = \delta\rho - 3\boldsymbol{j}\cdot\boldsymbol{j}/\rho_0, \quad m_3^{(\mathrm{eq})} = j_x, \tag{12b}$$

$$m_4^{(\mathrm{eq})} = -j_x, \quad m_5^{(\mathrm{eq})} = j_y, \quad m_6^{(\mathrm{eq})} = -j_y, \tag{12c}$$

$$m_7^{(\mathrm{eq})} = \left(j_x^2 - j_y^2\right)/\rho_0, \quad m_8^{(\mathrm{eq})} = j_x j_y/\rho_0, \tag{12d}$$

where $\boldsymbol{j} = \rho_0\boldsymbol{u} = (j_x, j_y)$ is the momentum.

2.2. Front tracking method

When equation (8), the evolution equation, is solved numerically on a stationary Eulerian grid, the density and viscosity on these grid points are required. Now we consider a two-phase flow: in each of two phases the flow is assumed to be incompressible, and the fluid parameters, such as density and viscosity, in each phase are taken to be constant. Hence the density and viscosity are physically discontinuous across the interface, and this discontinuity at grid points adjacent to the interface brings many difficulties to numerical methods. In order to effectively simulate the interface movement of two-phase flow, Tryggvason *et al.*[15] and Unverdi and Tryggvason[16] adopted a stationary Eulerian background grid to solve the governing equations of flow, and an additional moving Lagrangian grid to track explicitly the interface motion. In this paper, the entire flow domain is solved by just one evolution equation. An illustration of such a grid system is shown in Fig. 1.

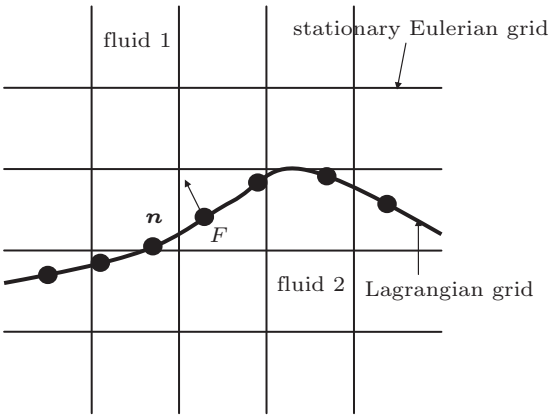

Fig. 1. The LBM-front tracking method with two grids: a stationary Eulerian grid for the flow field solved by the LBM model and a moving Lagrangian grid for tracking the interface.

At each time step t, we should determine the distributed material properties in the entire flow domain, where an indicator function $I(\boldsymbol{x}, t)$ is introduced. Let

this indicator function be zero in one phase and one in the other phase, and then we can define

$$b(\boldsymbol{x},t) = b_1 + (b_0 - b_1)\, I(\boldsymbol{x},t), \tag{13}$$

where $b(\boldsymbol{x},t)$ is either fluid density or viscosity, and the subscripts 0 and 1 refer to fluid one and fluid two, respectively. According to the interface location, the indicator function $I(\boldsymbol{x},t)$ is obtained by solving a Poisson equation

$$\boldsymbol{\nabla}^2 I = \boldsymbol{\nabla}\cdot\boldsymbol{G}, \tag{14}$$

where $\boldsymbol{G}$ contains the information about the interface and is expressed as

$$\boldsymbol{G} = \int_{\Gamma} \boldsymbol{n}_{\mathrm{f}} D(\boldsymbol{x}-\boldsymbol{x}_{\mathrm{f}})\,\mathrm{d}s, \tag{15}$$

where $\boldsymbol{n}_{\mathrm{f}}$ is the unit normal vector of the interface, Γ represents the interface, and $D(\boldsymbol{x}-\boldsymbol{x}_{\mathrm{f}})$ is a distribution function. In this paper, we adopt the traditional Peskin distribution function[14] to approximate the D function

$$D(\boldsymbol{x}-x_{\mathrm{f}}) = \begin{cases} (4h)^{-2}\prod\limits_{i=1}^{2}\left(1+\cos\dfrac{\pi}{2h}(x_i - x_{\mathrm{f},i})\right), & \text{if} \quad |x_i - x_{\mathrm{f},i}| < 2h\,, \\ 0, & \text{otherwise}, \end{cases} \tag{16}$$

where h is equal to the space constant δ_x. Equation (14) is solved by a standard second-order centered difference method, and the linear equation system is solved with a traditional Successive–Over–Relaxation method. Figure 2 illustrates the indicator function distribution.

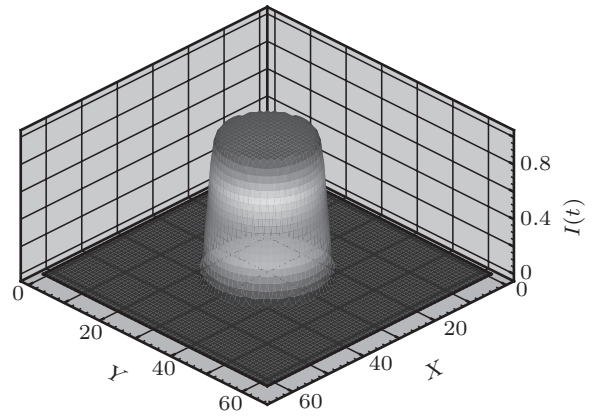

Fig. 2. Indicator function (1 inside the bubble, and 0 outside).

The interface maker points are moved in a Lagrangian manner

$$\frac{\mathrm{d}\boldsymbol{x}_{\mathrm{f}}}{\mathrm{d}t} = \boldsymbol{u}_{\mathrm{f}}, \tag{17}$$

where $\boldsymbol{u}_{\mathrm{f}}$ represents the velocity of the interface maker points which are interpolated from the flow field over the background grid

$$\boldsymbol{u}_{\mathrm{f}}(\boldsymbol{x}_{\mathrm{f}},t) = \sum_i \boldsymbol{u}(\boldsymbol{x}_i,t) D(\boldsymbol{x}_i - x_{\mathrm{f}})\,. \tag{18}$$

2.3. Surface tension

Accurate calculation of the surface tension is a great challenge of numerical methods for the multiphase flow model. In this paper, the surface tension is implemented directly from the normal vector and curvature of the Lagrangian interface and expressed as

$$\boldsymbol{F}_{\mathrm{f}} = \sigma k_{\mathrm{f}} \boldsymbol{n}_{\mathrm{f}} \Delta s_{\mathrm{f}}, \tag{19}$$

where σ is the surface tension, k_{f} is the curvature of the interface, and Δs_{f} is the distance between two adjacent maker points. According to Eq. (17) we can obtain the coordinates of the interface maker points, and then the interface is represented by the following vector parametric equation:

$$\boldsymbol{R}(v) = g(v)\,\boldsymbol{i} + h(v)\,\boldsymbol{j}, \tag{20}$$

where $g(v)$ and $h(v)$ are computed by fitting a four-order Lagrange polynomial

$$g(v) = \sum_{i=0}^{4} \mathrm{L}_i(v)\, x_{\mathrm{f}}(v_i), \tag{21a}$$

$$h(v) = \sum_{i=0}^{4} \mathrm{L}_i(v)\, y_{\mathrm{f}}(v_i), \tag{21b}$$

where

$$\mathrm{L}_i(v) = \prod_{\substack{j=0 \\ j\neq i}}^{4} \frac{v - v_j}{v_i - v_j}. \tag{22}$$

We can compute the normal vector and curvature at any point on the interface from the following formulas:

$$\boldsymbol{n}_{\mathrm{f}} = \frac{-h'\boldsymbol{i} + g'\boldsymbol{j}}{\sqrt{(g')^2 + (h')^2}}, \tag{23}$$

$$k_{\mathrm{f}} = \frac{g'h'' - g''h'}{\left((g')^2 + (h')^2\right)^{3/2}}, \tag{24}$$

where the prime denotes the differentiation with respect to parameter v; $\boldsymbol{i}$ and $\boldsymbol{j}$ are unit vectors in the x and y directions, respectively.

The surface tension is then distributed into the background grid in the same way as the interpolation of the velocity, and it is given as

$$\boldsymbol{F}(\boldsymbol{x}) = \sum_k \boldsymbol{F}_{\mathrm{f}}(\boldsymbol{x}_k)\, D(\boldsymbol{x} - x_k). \tag{25}$$

The coupling between the surface tension and flow is established by adding an external forcing term to the right-hand side of the evolution Eq. (8), the forcing term is expressed as[20]

$$\tilde{\boldsymbol{F}} = \boldsymbol{M}^{-1}\left(\boldsymbol{I} - \frac{1}{2}\tilde{\boldsymbol{S}}\right)\boldsymbol{M}\bar{\boldsymbol{F}}, \tag{26}$$

where $\boldsymbol{I}$ is the unit matrix, $\tilde{\boldsymbol{F}} = \left(\tilde{F}_0, \tilde{F}_1, \ldots, \tilde{F}_8\right)^{\mathrm{T}}$, and $\bar{\boldsymbol{F}} = \left(\bar{F}_0, \bar{F}_1, \ldots, \bar{F}_8\right)^{\mathrm{T}}$ is related to the surface tension $\boldsymbol{F}$

$$\underset{\alpha}{\bar{F}} = \omega_\alpha \left[\frac{\boldsymbol{e}_\alpha \cdot \boldsymbol{F}}{c_s^2} + \frac{\boldsymbol{u}F : \left(\boldsymbol{e}_\alpha \boldsymbol{e}_\alpha - c_s^2 \boldsymbol{I}\right)}{c_s^4}\right]. \tag{27}$$

In addition, equation (6) should be redefined as

$$\boldsymbol{u} = \frac{1}{\rho_0}\left(\sum_\alpha \boldsymbol{e}_\alpha f_\alpha + \frac{\delta_t}{2}\boldsymbol{F}\right). \tag{28}$$

In conclusion, each time step of the combined scheme consists of the following sub-steps.

(i) Interpolate the velocity $\boldsymbol{u}_{\mathrm{f}}$ of the interface marker points from the velocity $\boldsymbol{u}$ of the background fluid grid with Eq. (18).

(ii) Update the position of the interface marker points with Eq. (17).

(iii) Compute the surface tension from $\boldsymbol{x}_{\mathrm{f}}$ and then distribute the background fluid grid with Eqs. (19) and (25), respectively.

(iv) Compute the indicator function $I(\boldsymbol{x}, t)$ and update the material properties of the fluid.

(v) Compute the velocity field of the fluid with evolution Eqs. (5), (6), and (8).

(vi) Go back to the first sub-step and perform recomputation for the next time step.

3. Simulation and results

In this section, two test cases are considered to validate the algorithm and program. First, Laplace's law of surface tension is tested, and then the dispersion relation of the capillary wave between two fluids is simulated. The relaxation parameters in the collision matrix are chosen as, $s_0 = s_3 = s_5 = 1$, $s_1 = 1.1$, $s_4 = s_6 = 1.2$, $s_7 = s_8 = 1/\tau$, where τ is the relaxation time. For simplicity, the results are presented in the "lattice units".

3.1. Laplace's law of a bubble

To validate the presented numerical method for the two-phase flow, a verification test for Laplace's law is carried out. According to Laplace's law, the pressure difference between the interior and the exterior for a static bubble, $\Delta P = P_{\mathrm{in}} - P_{\mathrm{out}}$, is related to the surface tension σ and bubble radius R via the following formula:

$$\Delta P = P_{\mathrm{in}} - P_{\mathrm{out}} = \frac{\sigma}{R}, \tag{29}$$

where P_{in} and P_{out} are the pressures inside and outside of the bubble, respectively. As done in Ref. [2], the pressure inside the bubble is measured by averaging the pressure over all lattice points inside a circle of radius $0.7R$ and the outside pressure is measured by averaging the pressure over all lattice points away from $1.3R$ of the bubble centre.

A number of tests with bubble radii ranging from 14 to 22 lattice units and the values of surface tension σ from 0.001 to 0.01 are conducted. The lattice size is 151×151 and the periodic boundary conditions for all directions are used. As demonstrated in Fig. 3, the simulation results based on the method in the paper are consistent with the theoretical solutions, and the maximal relative error is less than 0.3%.

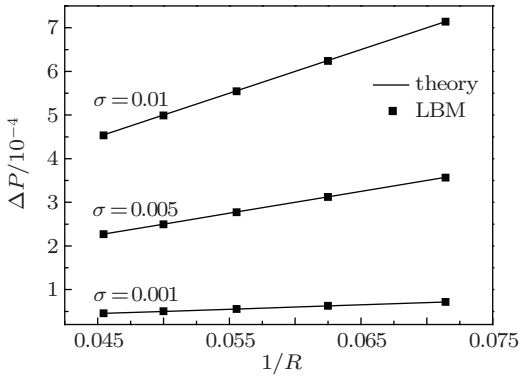

Fig. 3. Pressure differences across the interface for different bubble radii from LBM simulations (solid squares) and the theoretical solution based on the Laplace relationship Eq. (24) (solid line).

3.2. Capillary wave

The abovementioned test of Laplace's law verifies only the ability to simulate a stationary interface. To verify the capability of the model for a dynamical interface, the capillary wave is simulated. In this simulation, initially a single sinusoidal wave is set in the middle of the domain, with wavelength λ equal to the domain width. The initial wave amplitude h_0 of the perturbation is set to be $0.01N_y$ to satisfy the condition of long wavelength limit, where N_y is the domain length,

$$h\left(\boldsymbol{x}_{\mathrm{f}}, 0\right) = h_0 \cos\left(k\boldsymbol{x}_{\mathrm{f}}\right), \tag{30}$$

where $k = 2\pi/\lambda$ is wave number. For a small perturbation amplitude. When the kinematic viscosities are the same for both fluids, a theoretical solution for the wave amplitude $h\left(t\right)$ based on the normal mode analysis is derived[19] as

$$h\left(t\right) = h_0 \cos\left[\mathrm{Re}\left(\omega\right)t\right] \, \mathrm{e}^{-\mathrm{Im}(\omega)t}, \tag{31}$$

where the complex frequency ω is related to the wave number k through the dispersion relation[21]

$$\omega^2 = \frac{\sigma k^3 \left(1 - k/q\right)}{2\rho} \tag{32}$$

with

$$q = \sqrt{k^2 - \mathrm{i}\omega/\nu}. \tag{33}$$

By using Eqs. (32) and (33), one can find that q is a root of the quartic equation as

$$q\left(q-k\right)\left(q+k\right)^2 = -\frac{\sigma k^3}{2\nu^2\rho}, \tag{34}$$

which can be solved numerically.

To numerically study capillary wave, we carry out simulations on a square domain with a resolution of 151 × 151. A periodic boundary condition is adopted in the horizontal direction, while a nonslip wall boundary is used in the vertical direction. A number of tests with surface tension values ranging from 0.002 to 0.01 are conducted. Table 1 presents the simulated results obtained for the complex frequencies at different surface tension values, and the theoretical complex frequencies computed from Eqs. (32) and (33) are also shown in Table 1 for comparison. This table indicates that our results accord well with those theoretical solutions, and the relative errors are less than 0.6%. In order to study the dependence of the calculation on grid size, the numerical simulations for $\sigma = 0.01$ are conducted on five grids: 32 × 32, 64 × 64, 128 × 128, 151 × 151, and 256 × 256. The results are presented in Table 2, exhibiting clearly that the relative errors between the numerical results and theoretical solutions decrease from 4.956% to 0.231% with the increase of grid number, and the accuracy of the simulation with grid 151 × 151 is acceptable. The time evolution of the wave amplitude for $\sigma = 0.01$ is demonstrated in Fig. 4, and the numerical results (empty downward triangles) are in good agreement with the theoretical resolutions (solid line).

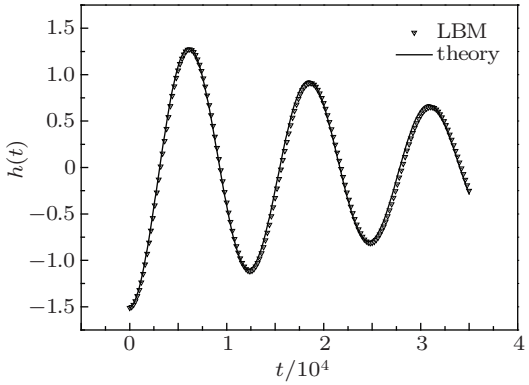

Fig. 4. Evolutions of the amplitude of the capillary wave with time: the LBM results (empty downward triangles) with grid 151 × 151 and the analytical solutions (solid line).

Table 1. Comparison of the oscillation frequency between the analytical solutions and the LBM results for different surface tension values.

σ	ω (MRT-FT)/10^{-4}	ω (Theory)/10^{-4}	Error
0.002	2.493	2.489	0.161%
0.004	3.550	3.558	0.225%
0.006	4.363	4.381	0.411%
0.008	5.067	5.077	0.197%
0.01	5.660	5.691	0.545%

Table 2. Grid dependence study of the capillary wave, comparison of the oscillation frequency between the analytical solutions and the LBM results.

Mesh	ω (MRT-FT)	ω (Theory)	Error
32×32	5.236×10^{-3}	5.509×10^{-3}	4.956%
64×64	1.964×10^{-3}	2.014×10^{-3}	2.483%
128×128	7.222×10^{-4}	7.264×10^{-4}	0.578%
151×151	5.660×10^{-4}	5.691×10^{-4}	0.545%
256×256	2.596×10^{-4}	2.602×10^{-4}	0.231%

4. Conclusions

We developed a lattice Boltzmann-front tracking method to investigate numerically two-phase flow

with interfacial dynamics and surface tension. An incompressible multi-relaxation-time lattice Boltzmann method was adopted, and an indicator function was introduced to update accurately the fluid properties. The accurate computation of the surface tension has been a challenge of numerical simulation for the dynamical interface for a long time. In this paper, the interface was tracked explicitly by the front tracking method, and a four-order Lagrange polynomial is adopted to compute accurately the surface tension. Two verification tests were conducted for both static interface and dynamical interface, and our results are in good agreement with theoretical solutions, which implies that both the method and program developed in the paper are applicable with high precision for the two-phase flow with shape dynamical interface, where the surface tension is implemented accurately.

Acknowledgement

The authors are grateful to the staff of the Centre for Computer Materials Science at the Institute for Materials Research, Tohoku University, for their continuous support of the SR8000-G1/64 supercomputing facilities.

References

[1] Hirt C W and Nichols B D 1981 *J. Comput. Phys.* **39** 201
[2] Ruschak K J 1980 *Int. J. Numer. Methods Eng.* **15** 639
[3] Sussman M, Smereka P and Osher S 1994 *J. Comput. Phys.* **114** 146
[4] Chen S and Doolen G D 1998 *Ann. Rev. Fluid Mech.* **30** 329
[5] Gunstensen A K, Rothman D H, Zaleski S and Zanetti G 1991 *Phys. Rev.* A **43** 4320
[6] Shan X W and Chen H D 1993 *Phys. Rev.* E **47** 1815
[7] Swift M R, Orlandini E, Osborn W R and Yeomans J M 1996 *Phys. Rev.* E **54** 5041
[8] Yi H H, Yang X F, Wang C F and Li H B 2009 *Chin. Phys.* B **18** 2878
[9] Yi H H, Fan L J, Yang X F and Li H B 2009 *Chin. Phys. Lett.* **26** 048701
[10] Cai J and Huai X L 2009 *Chin. Phys. Lett.* **26** 064401
[11] Zhong C W, Xie J F, Zhou C S, Xiong S W and Yin D C 2009 *Chin. Phys.* B **18** 4083
[12] Ran Z 2009 *Chin. Phys.* B **18** 2159
[13] Lallemand P, Luo L S and Peng Y 2007 *J. Comput. Phys.* **226** 1367
[14] Peskin C S 1977 *J. Comput. Phys.* **2**5 220
[15] Tryggvason G, Bunner B, Esmaeeli A, Juric D, Rawahi N, Tauber W, Han J, Nas S and Jan Y J 2001 *J. Comput. Phys.* **169** 708
[16] Unverdi S O and Tryggvason G 1992 *J. Comput. Phys.* **100** 25
[17] He X Y and Luo L S 1997 *J. Stat. Phys.* **88** 927
[18] Lallemand P and Luo L S 2000 *Phys. Rev.* E **61** 6546
[19] D'Humières D 1992 *Progress in Astronautics and Aeronauttics* **159** 450
[20] Guo Z L and Zheng C G 2008 *Int. J. Comput. Fluid Dyn.* **22** 465
[21] Popinet S and Zaleski S 1999 *Int. J. Numer. Methods Fulids* **30** 775